JOURNAL OF RAMAN SPECTROSCOPY, VOL. 18, 561-568 (1987)

Measurement of Raman Scattered Intensities in Media with Natural or Field-Induced Optical Activity

A. V. Slobodyanyuk* and G. Schaack†
Physikalisches Institut der Universität Würzburg, D-8700 Würzburg, FRG

The intensity of Raman scattered light has been calculated for gyrotropic media, i.e. for media with a natural optical activity or a gyrotropy induced by a magnetic field. It is shown that anomalies in the scattered intensity are in general due to interference effects between the two orthogonally polarized normal modes of electromagnetic radiation propagating in the anisotropic crystal either in the incident or in the scattered beam or in both. Only when the state of polarization of the incident and the scattered waves agrees with one of these normal modes are clear results obtained which are simply to interpret. Hence the intensity anomalies sometimes observed in these media find an interpretation in the frame of the generally accepted theory. No breakdown of selection rules will occur in such media.

The calculated results are compared with experimental findings in α-quartz and in ZnP_2 and also in paramagnetic $TmVO_4$ and in CeF_3 in external magnetic fields.

INTRODUCTION

The prime task of Raman spectroscopy, irrespective of any specific physical application, is the measurement of the frequency dependence of elements of the Raman tensor. In most cases these measurements are performed using light with a well defined state of polarization, in general linear polarization. The observed Raman intensity (the scattering efficiency), ${}^{\mu}I$, is calculated using[1]

$$ {}^{\mu}I = c \left| \sum_{i,j} e_i^{\mathrm{I}} \, {}^{\mu}A_{ij} \, e_j^{\mathrm{S}} \right|^2 \qquad (1) $$

where ${}^{\mu}A_{ij}$ are components of the Raman tensor for an excitation μ at a frequency ${}^{\mu}\Omega$, e_i^{I} and e_j^{S} are components i, j of unit vectors of polarization of the electric vector of incident and scattered light, respectively, and $i, j = x, y, z$. It is assumed implicitly that the polarization states of incident and scattered light remain constant while propagating in the scattering medium:

$$ \frac{\mathrm{d}\mathbf{e}^{\mathrm{I}}}{\mathrm{d}r} = 0, \frac{\mathrm{d}\mathbf{e}^{\mathrm{S}}}{\mathrm{d}r'} = 0 \qquad (2) $$

where $\mathrm{d}r$ and $\mathrm{d}r'$ are elements of the path of incident or scattered light.

Assumption (2) is not always fulfilled: in gyrotropic media‡ the polarization of incoming or scattered light may change while propagating through the crystal. If, as is well known, the light propagates through an isotropic or cubic gyrotropic medium or if the wavevector $\mathbf{k}$ of the light is oriented parallel to the optical axis in a uniaxial or biaxial gyrotropic crystal, a rotation of the plane of polarization of linear polarized light is observed. For general directions of $\mathbf{k}$ in the presence of ordinary birefringence different states of elliptic polarization will be observed[3] when linearly polarized light enters the crystal. This fact is the main source of experimental problems and of many erroneous interpretations of spectra from gyrotropic media in the existing literature.[4] In Ref. 4 it was claimed that as a consequence of Faraday rotation in magnetic materials selection rules for phonon Raman scattering will break down. New selection rules were formulated, which depend on the size of the sample under study and have no clear physical sense. In other publications,[5-7] the problems of gyration have been recognized but evaded or solved only in an unsatisfactory manner, i.e. by using scattering geometries, where the linear birefringence dominates over gyrotropy or by reducing the pathlength of the light in the crystal at the expense of the size of the signal in order to neglect gyration.

A rigorous approach to this problem is to use vectors of polarization for the incoming and scattered light which are eigenstates of the wave equation for electromagnetic waves in the medium[3] and which by definition satisfy conditions (2). In gyrotropic media circularly polarized light should be used accordingly in suitable geometries or the scattered light should be analysed for circular components whenever linear birefringence is absent. Equation (1) can be used to calculate the Raman scattering efficiency provided that the components A_{ij} have been transformed to a suitable basis of eigenstates (e.g. circular). The effects of using circularly polarized radiation in gyrotropic media have been discussed for specific examples in crystals showing natural optical activity[8-11] and in uniaxial paramagnetic crystals in external magnetic fields parallel to the optical axis.[12,13]

In this paper it will be shown that in gyrotropic media the intensity of phonon Raman scattering can depend

* Permanent address: Department of Physics, T.G. Schevchenko State University, 252127 Kiev, USSR.

† Author to whom correspondence should be addressed.

‡ Media which demonstrate either natural optical activity or field-induced activity either by a magnetic field (Faraday effect) or an electric field (electrogyration).[2]

0377-0486/87/080561-08 $05.00

Received 22 September 1986
Accepted 4 May 1987

considerably on the condition of observation, but there is no violation of selection rules in an external magnetic field other than predicted by the application of Curie's principle (the point group of the crystal in a homogeneous magnetic field—the point group of the latter is $C_{\infty h}$— is the subgroup comprising all the symmetry elements common to the point group of the crystal and to $C_{\infty h}$). Effects in magnetically ordered systems, which have to be treated by the application of Shubnikov groups,[14] will not be dealt with here.

In the next section the Raman intensity will be calculated for the case where the incident wave or the scattered wave selected by the analyser are not eigenstates of the crystal under study. It will be shown that anomalies of the Raman intensity are due to interference because of the simultaneous effect of two orthogonal incoming or scattered waves with well defined phase relations between them. In the Experimental Results section some specific examples are discussed for the most often applied 90° scattering geometry and pertinent experimental results for α-quartz and $TmVO_4$ are presented. The final section outlines a general discussion of the relevance of our results and the most important conclusions are given.

CALCULATION OF RAMAN INTENSITIES

If laser light of the general polarization state $\mathbf{e}^{\mathrm{I}}$ and wavevector $\mathbf{k}_n^{\mathrm{I}}$ is entering a non-absorbing crystal with the polarization of the two normal waves $\mathbf{e}_n$ (wavevector $\mathbf{k}_n$), $\mathbf{e}_{\tilde{n}}$ ($\mathbf{k}_{\tilde{n}}$), then $\mathbf{e}^{\mathrm{I}}$ will decompose into these normal waves:

$$\mathbf{e}^{\mathrm{I}} = a_n \mathbf{e}_n + a_{\tilde{n}} \mathbf{e}_{\tilde{n}} \tag{3a}$$

with the complex amplitudes $a_{n,\tilde{n}} = \mathbf{e}^{\mathrm{I}} \cdot \mathbf{e}^*_{n,\tilde{n}}$ of the normal waves n, $\tilde{n}$. The scattered normal waves $\mathbf{e}_{n'}$ in direction $\mathbf{k}_{n'}$ and ($\mathbf{e}_{\tilde{n}'}$, $\mathbf{k}_{\tilde{n}'}$) enter the analyser A [set for state $(\mathbf{e}^{\mathrm{S}})_{\mathrm{A}}$] and the projections $(a_{n'})_{\mathrm{A}}\,(e^{\mathrm{S}})_{\mathrm{A}}$ and $(a_{\tilde{n}'})_{\mathrm{A}}(e^{\mathrm{S}})_{\mathrm{A}}$ of these amplitudes are transmitted to the spectrograph, while the orthogonal components $(a_{n'})_{\perp}(e^{\mathrm{S}})$ and $(a_{\tilde{n}'})_{\perp}(e^{\mathrm{S}})$ are eliminated:

$$\begin{aligned} \mathbf{e}_{n'} &= (a_{n'})_{\mathrm{A}}(\mathbf{e}^{\mathrm{S}})_{\mathrm{A}} + (a_{n'})_{\perp}(\mathbf{e}^{\mathrm{S}})_{\perp}; \\ e_{\tilde{n}'} &= (a_{\tilde{n}'})_{\mathrm{A}}(e^{\mathrm{S}})_{\mathrm{A}} + (a_{\tilde{n}'})_{\perp}(\mathbf{e}^{\mathrm{S}})_{\perp}; \end{aligned} \tag{3b}$$

The amplitude of the detected light, originating from one unit cell (molecule) l and scattered in direction $\mathbf{k}_{n'}$, is (cf. Fig. 1)

$$\begin{aligned} {}^{l}E^{\mu}(\mathbf{r}_0) = c \sum_{n,n'} |{}^{l}E^{\mu}_{nn'}| \exp\{i[\omega t \mp {}^{\mu}\Omega t - \mathbf{k}_n \mathbf{r}_l \\ - \mathbf{k}_{n'}(\mathbf{r}_0 - \mathbf{r}_1) + {}^{\mu}\Phi_1 + \phi_n + \phi_{n'}]\} \end{aligned} \tag{4}$$

where

$$|{}^{l}E^{\mu}_{nn'}| = \left| \sum_{i,j} a_n(\mathbf{e}_n)_i \, {}^{\mu}A_{ij} (a_{n'})_{\mathrm{A}} (e^{\mathrm{S}})_{\mathrm{A},j} \right|$$

where ω is the frequency of the incident light ($\mathbf{k}_n$), the scattered wave ($\mathbf{k}_{n'}$) oscillates with the frequency $\omega \mp {}^{\mu}\Omega$; ϕ_n, $\phi_{n'}$, ${}^{\mu}\Phi_1$ are initial phases of normal waves n and n' and of vibration μ in l. $\mathbf{r}_1$ is a vector from the origin to the scattering centre l, $\mathbf{r}_0$ indicates the position of the detector, where the scattered amplitude or intensity has to be calculated (Fig. 1). The constant c comprises all the other (essentially geometric) factors, determining the amplitude E, which are of no concern to the present problem.

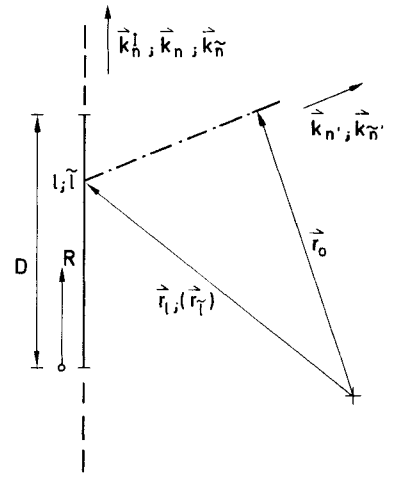

Figure 1. Scattering geometry. D, Part of the illuminated sample focused on the entrance slit of the monochromator; l, $\tilde{l}$, scattering centres at r_l, $r_{\tilde{l}}$ or at R; k^{I}_n, wavevector of incident laser radiation; k_n, $k_{\tilde{n}}$, wavevectors of the two eigenmodes of the laser radiation in the crystal; $k_{n'}$, $k_{\tilde{n}'}$, wavevectors of the eigenmodes of scattered radiation. Detector of scattered radiation at r_0.

In the following, the calculation of the observed intensity will be presented in some detail (cf. Refs 15 and 16) for ease of control. The intensity ${}^{\mu}I$ will be calculated for an extended scattering volume of dimensions $D \gg \lambda$, containing many scattering centres l, where the interference between normal waves (e_n, $\mathbf{k}_n$) ($\mathbf{e}_{n'}$, $\mathbf{k}_{n'}$) is considered explicitly (see also Ref. 11).

$$\begin{aligned} {}^{\mu}I(\mathbf{r}_0) &= c' \sum_{l\tilde{l}} ({}^{l}E^{\mu})({}^{\tilde{l}}E^{\mu})^* \\ &= c' \sum_{l,\tilde{l}} \sum_{\substack{n,\tilde{n}, \\ n',\tilde{n}'}} |{}^{l}E^{\mu}_{n,n'}| \, |{}^{\tilde{l}}E^{\mu}_{\tilde{n},\tilde{n}'}| \\ &\quad \times \exp\{i[\mathbf{k}_n \mathbf{r}_l - \mathbf{k}_{\tilde{n}} \mathbf{r}_{\tilde{l}} + \mathbf{k}_{n'}(\mathbf{r}_0 - \mathbf{r}_l) - \mathbf{k}_{\tilde{n}'}(\mathbf{r}_0 - \mathbf{r}_{\tilde{l}}) \\ &\quad + \phi_n - \phi_{\tilde{n}} + \phi_{n'} - \phi_{\tilde{n}'} + {}^{\mu}\Phi_l - {}^{\mu}\Phi_{\tilde{l}}]\} \end{aligned} \tag{5}$$

The subscripts $\tilde{l}$, $\tilde{n}$ and $\tilde{n}'$ indicate that normal waves n' or $\tilde{n}'$ will interfere, which originate from different scattering centres, as well as different normal waves n, $\tilde{n}$; n', $\tilde{n}'$ starting at the same centre.

It is convenient to rewrite Eqn (5) in the following form:

$$\begin{aligned} {}^{\mu}I(\mathbf{r}_0) &= c' \sum_{l=\tilde{l}} \sum_{\substack{n,\tilde{n}, \\ n',\tilde{n}'}} |{}^{l}E^{\mu}_{nn'}| \, |{}^{l}E^{\mu}_{\tilde{n}\tilde{n}'}| \\ &\quad \times \exp\{i[(\mathbf{k}_n - \mathbf{k}_{\tilde{n}})\mathbf{r}_l + (\mathbf{k}_{n'} - \mathbf{k}_{\tilde{n}'})(\mathbf{r}_0 - \mathbf{r}_l) \\ &\quad + \phi_n - \phi_{\tilde{n}} + \phi_{n'} - \phi_{\tilde{n}'}]\} \\ &\quad + 2c' \sum_{l,\tilde{l}<l} \sum_{\substack{n,\tilde{n}, \\ n',\tilde{n}'}} |{}^{l}E^{\mu}_{nn'}| \, |{}^{\tilde{l}}E^{\mu}_{\tilde{n}\tilde{n}'}| \\ &\quad \times \cos[\mathbf{k}_n \mathbf{r}_l - \mathbf{k}_{\tilde{n}} \mathbf{r}_{\tilde{l}} + \mathbf{k}_{n'}(\mathbf{r}_0 - \mathbf{r}_l) - \mathbf{k}_{\tilde{n}'}(\mathbf{r}_0 - \mathbf{r}_{\tilde{l}}) \\ &\quad + \phi_n - \phi_{\tilde{n}} + \phi_{n'} - \phi_{\tilde{n}'} + {}^{\mu}\Phi_l - {}^{\mu}\Phi_{\tilde{l}}] \end{aligned} \tag{5a}$$

For internal vibrations in gases and liquids, the second term in Eqn (5a) sums to zero because of the randomness of the phases ${}^{\mu}\Phi_l$ and ${}^{\mu}\Phi_{\tilde{l}}$. For crystals with non-local-

ized excitations (phonons μ with wavevector ${}^{\mu}\mathbf{k}_p$), i.e. if a spatial correlation exists between the phases in different unit cells according to

$$ {}^{\mu}\Phi_l - {}^{\mu}\Phi_{\tilde{l}} = \pm {}^{\mu}\mathbf{k}_p(\mathbf{r}_l - \mathbf{r}_{\tilde{l}}) \tag{6} $$

the argument of the cosine function in the second term of Eqn (5a) can be identically zero (and only in this case this term will contribute) if

$$ \mathbf{k}_n - \mathbf{k}_{n'} \pm {}^{\mu}\mathbf{k}_p = 0; \quad \mathbf{k}_{\tilde{n}} = \mathbf{k}_n, \mathbf{k}_{\tilde{n}'} = \mathbf{k}_{n'} \tag{7} $$

(conservation of wavevectors for either Stokes or anti-Stokes processes). In the general case of an extended medium, however, the contributions due to waves from different origins and from different normal waves will again cancel out the second term in Eqn (5a) (i.e. $\mathbf{k}_n$ and $\mathbf{k}_{n'}$ and thus $\mathbf{k}_p$ are not strictly defined) and we can concentrate on the first term only.

In this case, which is of practical interest, the spatial coherence is neglected and only the temporal coherence is taken into account. The scattered intensity considered originates from one 'point' l, but depends on the position of this point and on the parameters of the normal waves of both the incident and scattered light. The physical meaning of this becomes especially clear if ${}^{\mu}I_l(\mathbf{r}_0)$ is decomposed into four terms:

$$ \begin{aligned} {}^{\mu}I_l(\mathbf{r}_0) = c' \Bigg\{ & \sum_{\substack{n=\tilde{n};\\ n'=\tilde{n}'}} |E_{nn'l}|^2 \\ & + 2 \sum_{\substack{n,\tilde{n};\\ n'=\tilde{n}'}} |E_{nn'}|\,|E_{\tilde{n}n'}| \cos\left[(k_n - k_{\tilde{n}})R_l + \phi_n - \phi_{\tilde{n}}\right] \\ & + 2 \sum_{\substack{n',\tilde{n}';\\ n=\tilde{n}}} |E_{nn'}|\,|E_{n\tilde{n}'}| \cos\left[(k_{n'} - k_{\tilde{n}'})r_l + \phi_{n'} - \phi_{\tilde{n}'}\right] \\ & + 2 \sum_{\substack{n,\tilde{n};\\ n',\tilde{n}'}} |E_{nn'}|\,|E_{\tilde{n}\tilde{n}'}| \cos\left[(k_n - k_{\tilde{n}})R_l\right. \\ & \left. + (k_{n'} - k_{\tilde{n}'})r_l + \phi_n - \phi_{\tilde{n}} + \phi_{n'} - \phi_{\tilde{n}'}\right] \Bigg\} \end{aligned} \tag{8} $$

In this expression the scattering centre l is defined through its position described by R_l and r_l, the distances of l from the reference planes of phases of incoming or scattered wave, respectively (Fig. 1). For simplicity these planes should coincide with sample faces. The first term in Eqn (8) is the contribution to the total intensity due to scattering processes from one incident normal wave n into a single scattered normal wave n'. In this most simple case Eqn (8) reduces to Eqn (1). The second term is due to interference effects between two incident normal waves scattering into the same normal wave n' and the third term gives the modulation due to interference between two scattered normal waves fed by a single incident wave. The last term gives the additional contributions if both incident and scattered waves have to be decomposed each into two normal waves of the material.

The signal W detected by the spectrometer is thus

$$ {}^{\mu}W = b \int_S \int_D {}^{\mu}I_l(R, r)\, \mathrm{d}s\, \mathrm{d}R \tag{9} $$

where S is the effective cross-section of the laser beam, D is defined in Fig. 1, b is constant. It should be noted that modulation effects due to the last three terms in Eqn (8) are non-negligible if D is comparable to the coherence length $L_{\mathrm{coh}} = \lambda/2\Delta n$, where Δn is the difference of the refractive indices of both normal waves, propagating either along k_n or $k_{n'}$ (double refraction). One can neglect the contribution of these terms if $D \ll L_{\mathrm{coh}}$ (reducing the pathlength of the light as mentioned above) or if $L_{\mathrm{coh}} \ll D$, when this contribution will be averaged out (see below).

EXPERIMENTAL RESULTS

To demonstrate the different aspects of Eqns (8) and (9) experimentally, we investigated Raman scattering in trigonal (D_3) α-quartz with a natural optical activity of $\rho = 29.3°\ \mathrm{mm}^{-1}$ ($\lambda = 514$ nm) and in the tetragonal paramagnet thulium vanadate [$TmVO_4$ (D_{4h})], which performes a structural phase transition at $T_D = 2.14$ K to an orthorhombic phase (D_{2h}) due to the cooperative Jahn-Teller effect.[17] Both experiments were performed with and without an external magnetic field B parallel to the optical axis $\hat{Z}$ of the crystals.

The experimental set-up is shown in Fig. 2. The radiation of an Ar^+ laser was polarized either linearly or circularly and propagated in the sample along $\hat{Z}$. The scattered light was collected (90° geometry) by a condenser ($f = 20$ cm) and focused (1:1) on the entrance slit of the double monochromator, where a variable diaphragm was used to stop down the image of the scattering zone of the crystal. The polarization analyser could be mounted for the observation of either linearly or circularly polarized radiation.[13] The magnetic field ($B \leq 7$ T) was produced by a superconducting split-coil magnet system and the probes were immersed in superfluid helium whenever possible.

α-Quartz

We used a $10 \times 10 \times 10\ \mathrm{mm}^3$ cube with two faces cut normal to $\hat{Z}$. The two normal waves propagating parallel to $\hat{Z}$ have orthogonal circular polarization. If the laser light entering the crystal ($k_L \| \hat{Z}$) is linearly polarized, both partial waves n, $\tilde{n}$ have the same amplitude, but their relative phases vary, depending on the orientation of the plane of polarization in the XY plane of the light entering the crystal.

In the first experiment the analyser was set to detect either one of the two linearly polarized normal waves of the scattered light [$(\mathbf{e}^{\mathrm{S}}_{n'})_{\perp}\hat{Z}, (E), (\mathbf{e}^{\mathrm{S}}_{\tilde{n}'}) \| Z, (A_1)$]. Under

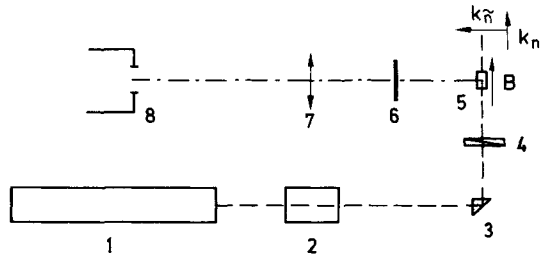

Figure 2. Experimental arrangement: 1 = argon laser ($\lambda = 514.5$ nm); 2 = tunable filter; 3 = deflecting prism; 4 = Soleil–Babinet compensator, 5 = sample (in magnetic field $B \leq 7$ T and immersed in superfluid helium if necessary), 6 = Polaroid analyser (linear or circular), 7 = condensor; 8 = entrance slit of double monochromator with diaphragm limiting the effective size of the sample.

this condition the intensity ${}^{\mu}I_l$ entering Eqn (9) is [from Eqn (8)]

$$
\begin{aligned}
{}^{\mu}I_l(R) = c'\Bigg\{ & \sum_{\substack{n=\tilde{n};\\ n'=\tilde{n}'}} |E_{nn'}|^2 \\
& + 2 \sum_{\substack{n>\tilde{n};\\ n'=\tilde{n}'}} |E_{nn'}||E_{\tilde{n}n'}| \cos\left[(k_n - k_{\tilde{n}})R + \phi_n - \phi_{\tilde{n}}\right]\Bigg\} \\
= c'\Bigg\{ & |a_n|^2 \left|\sum_{i,j} (e^n)_i \, {}^{\mu}A_{ij} (e^{\mathrm{S}}_{n'})_j\right|^2 \\
& + |a_{\tilde{n}}|^2 \left|\sum_{i,j} (e^{\tilde{n}})_l \, {}^{\mu}A_{ij} (e^{\mathrm{S}}_{n'})_j\right|^2 \\
& + 2|a_n|\,|a_{\tilde{n}}| \left|\sum_{i,j} (e^n)_i \, {}^{\mu}A_{ij} (e^{\mathrm{S}}_{n'})_j\right| \\
& \times \left|\sum_{i,j} (e^{\tilde{n}})_i \, {}^{\mu}A_{ij} (e^{\mathrm{S}}_{n'})_j\right| \\
& \times \cos\left[(k_n - k_{\tilde{n}})R + \phi_n - \phi_{\tilde{n}}\right]\Bigg\} \qquad (10)
\end{aligned}
$$

where $\mathbf{e}^n = (\mathbf{e}_x + i\mathbf{e}_y)\cdot 2^{-1/2}$; $\mathbf{e}^{\tilde{n}} = (\mathbf{e}_x - i\mathbf{e}_y)\cdot 2^{-1/2}$, $|a_n|$ and $|a_{\tilde{n}}|$ are the amplitudes of these waves and $\Delta\phi = \phi_n - \phi_{\tilde{n}}$ is the initial phase difference between these normal waves at the sample boundary as discussed above. Performing the integration (9) from R_1 to R_2, we have

$${}^{\mu}W = bW_0\left[1 + (A^2 + B^2)^{1/2} \sin\left(\Delta\phi + \arctan\frac{A}{B}\right)\right] \qquad (11)$$

where

$$W_0 = 2|a_n|^2 \left|\sum_{i,j} (e^n)_i \, {}^{\mu}A_{ij} (e^{\mathrm{S}}_{n'})_j\right|^2$$

$$A = \sin(\Delta k R_2) - \sin(\Delta k R_1)$$

$$B = \cos(\Delta k R_2) - \cos(\Delta k R_1)$$

and

$$\Delta k = k_n - k_{\tilde{n}}$$

For A = constant and B = constant, a sinusoidal dependence of ${}^{\mu}W$ is observed for varying $\Delta\phi$ (Fig. 3).

On applying an external magnetic field $\mathbf{B} \| \hat{Z}$, the wavevectors of the circular normal waves change due to the Faraday effect, which is superimposed to the natural optical activity according to[3]

$$\Delta k(B_z) = k_n(B_z) - k_{\tilde{n}}(B_z) = \frac{2\pi}{\lambda_0}\frac{1}{\bar{n}}(G_{zz} + F_{zz}B_z) \qquad (12)$$

where $\bar{n} = (n_n + n_{\tilde{n}})/2$, G_{zz} is the zz component of the gyration tensor and F_{zz} is the factor governing the Faraday rotation, which is directly proportional to the Verdet constant V. In Fig. 3 the change of Raman scattered intensity ${}^{\mu}W$ at $B = 7$ T is also plotted. The observed angular shift ${}^{\mu}W(B = 7\text{ T}) - {}^{\mu}W(B = 0)$ of 23° is just the value calculated from Verdet's constant for crystalline quartz:[18] $V(\lambda = 514\text{ nm}) \approx 3.3°\,\text{T}^{-1}\,\text{cm}^{-1}$.

Another illustrative example is provided by the E mode in α-quartz near 400 cm^{-1} with an LO-TO splitting of 8 cm^{-1}.[7] In Fig. 4(a) the scattering vectors with respect to the coordinate system of the crystal are shown. In this geometry a pure transversly polarized E' phonon is observed (component of the scattering tensor A_{xz}) and one oblique (pseudo-longitudinal) E'' phonon (A_{yz}). As $A'_{xz} = -A''_{yz} = e$,[1] a phase difference $\delta = \pi$ between the

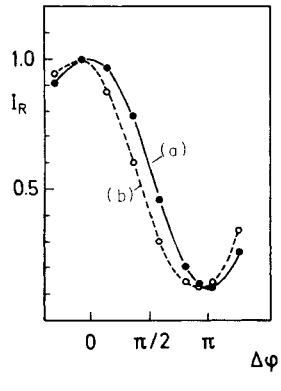

Figure 3. Normalized Raman intensity, I_R, of the 466 cm^{-1} line in α-quartz (A_1) depending on the initial phase difference $\Delta\varphi$ of circularly polarized normal waves; $T = 1.6$ K. (a) $B = 0$ T; (b) $B = 7$ T.

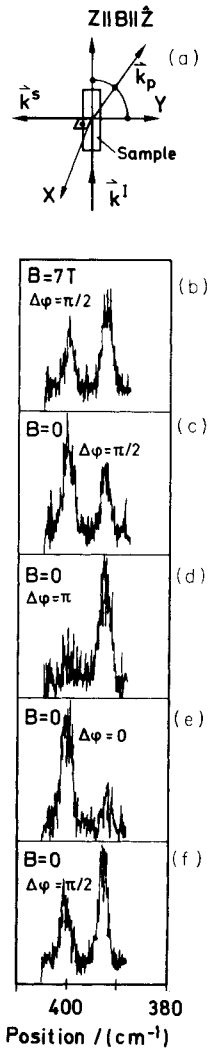

Figure 4. E doublet (TO–LO, 393–401 cm^{-1}) in α-quartz under different experimental conditions (magnetic field B, applied parallel to optical axis $\hat{Z}$, and initial phase differences $\Delta\varphi$ of the circular normal waves). (a) Scattering kinematics: k^i, k^S and k_p, wavevectors of incident, scattered light and Stokes phonon, respectively. Length of entrance slit: (b–e) 2 mm; (f) 6 mm. $T = 1.6$ K.

two tensor components enters the expression (11), which otherwise applies here in addition to the case of A modes:

$$
\begin{aligned}
{}^{E'}W &\propto W_0\left[1+(A^2+B^2)^{1/2}\sin\left(\Delta\phi+\arctan\frac{A}{B}\right)\right] \\
{}^{E''}W &\propto W_0\left[1+(A^2+B^2)^{1/2}\sin\left(\Delta\phi+\delta+\arctan\frac{A}{B}\right)\right]
\end{aligned}
\qquad (13)
$$

The Raman intensities of both transverse and longitudinal modes for specific values $\Delta\phi$ can be found in Fig. 4, where the B dependence following Eqn (12) is also demonstrated (Fig. 4(e)). We have also studied the E line at 128 cm^{-1} where the LO-TO splitting (0.04 cm^{-1})[19] is not resolved. No variation of ${}^{E}W$ is observed here by varying $\Delta\phi$ as the two contributions (13) just add up to a value ${}^{E}W$ which is independent of $\Delta\phi$. Figure 4(f) as compared with Fig. 4(c) is an example of the dependence of ${}^{E}W$ on $R_1 - R_2$ [sample length, see Eqn (12)]. Only the width of the diaphragm 8 (Fig. 2) was varied, all other conditions remaining unchanged. The variation of intensity with R_0 has been observed recently by Grishchuk and Slobodyanyuk (to be published).

It is worth mentioning that all intensity variations discussed above do not occur when the spectra are excited by only a single normal wave (right or left circularly polarized radiation).

Thulium Vanadate

The Tm^{3+} ion in paramagnetic $TmVO_4$ has a two-fold degenerate electronic ground state (g-factors: $g_{\hat{Z}} = 10.2$, $g_{\perp} \approx 0$).[17] $TmVO_4$ therefore comes close to an ideal Ising system. A strong Faraday rotation is induced by a magnetic field $\mathbf{B} \| \hat{Z}$ and for $\mathbf{k} \| \hat{Z}$ there are two circularly polarized normal waves. The temperature T of the probe ($4 \times 6 \times 10$ mm^3) was selected to ensure that the crystal is in the tetragonal high-temperature phase ($T > T_D = 2.14$ K) by adjusting the helium vapour pressure and the power of the incident laser beam properly. This could be controlled easily during the experiment by observing the conoscopic interference fringes in the laser beam after crossing the crystal.[17]

We investigated a group of three Raman lines of different types of symmetry: (A_{1g}, 899 cm^{-1}; B_{1g}, 823 cm^{-1}; E_g, 843 cm^{-1}). To observe all three lines simultaneously, the analyser was adjusted to be intermediate between $\mathbf{E} \| \hat{Z}$ and $\mathbf{E} \perp \hat{Z}$. Two normal waves of scattered light were thus detected but, owing to strong linear birefringence of $TmVO_4$, the contributions of the last two terms in Eqn (8) are averaged out and only the first two terms contribute.

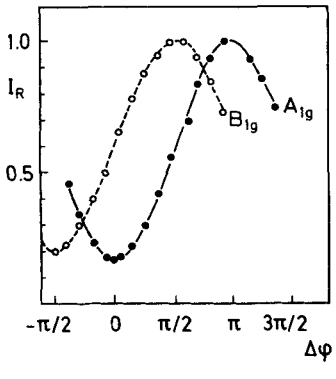

Figure 5. Dependence of normalized intensities of A_{1g} (899 cm^{-1}) and B_{1g} (823 cm^{-1}) lines in $TmVO_4$ on the initial phase difference $\Delta\varphi$.

Without a magnetic field $\mathbf{B} \| \hat{Z}$, the states of polarization of normal waves propagating parallel to $\hat{Z}$ are not strictly defined,[20] but it is advisable to assume circularly polarized waves as normal waves even at $B = 0$ T. Using the circular Raman tensors of Ovander[21] or the relationships given by Placzek[22] to transform the scattering tensor $A^l_{i,j}$ from a linear (l) basis x, y, z to a circular (c) basis: x^+, $(\xi) = (x + iy)2^{-1/2}$; x^-, $(\eta) = (x - iy)2^{-1/2}$, z, we obtain for the irreducible representations (i.r.) A_{1g}, B_{1g}

$$
(A_{1g}):\ A^c_{l,m} = \begin{pmatrix} 0 & a & 0 \\ a & 0 & 0 \\ 0 & 0 & b \end{pmatrix},
$$

$$
(B_{1g}):\ A^c_{l,m} = \begin{pmatrix} 0 & c & 0 \\ -c & 0 & 0 \\ 0 & 0 & 0 \end{pmatrix}
$$

starting from (A_{1g}) $A^l_{xx} = A^l_{yy} = a$, $A^l_{zz} = b$; and (B_{1g}) $A^l_{xx} = -A^l_{yy} = c$, $A^l_{zz} = 0$.[1]

If the y-component of the scattered light ($\mathbf{k}' \perp \hat{Z}$) is detected, we find

$$
\begin{aligned}
A_{1g}&: y' = ay \\
B_{1g}&: y' = cx
\end{aligned}
\qquad (15)
$$

To find the dependence of the scattered intensity on the phase difference $\phi_n - \phi_{\tilde{n}}$, i.e. from the orientation of the polarization plane of the incident light, we can again use Eqn (9) and find as before a sinusoidal variation ${}^{\mu}W(\Delta\phi)$ (Fig. 5). The two i.r.s differ, however, by a phase shift $\Delta\phi = \pi/2$, i.e. the scattered intensity has reached its maximum when the E vectors of incident and scattered light are collinearly (A_{1g}) or perpendicularly (B_{1g}) oriented with respect to each other. This experimental observation is clearly interpreted by the result [Eqn (15)] of our calculation. The intensity of the E_g line again does not depend on $\Delta\phi = \phi_n - \phi_{\tilde{n}}$.

In a paramagnetic crystal the coherence length depends on the magnetic field and decreases with increasing field strength. Accordingly, the interference effects will essentially determine the Raman scattered intensity at magnetic fields where the coherence length, L_{coh}, and the effective sample length, D, as determined by the diaphragm are of similar size but will lose their role when $L_{coh} \ll D$. In practice, the observed intensities will be dependent on B for small fields but become independent of B for high fields. This is illustrated in Fig. 6 for the A_{1g} line (899 cm^{-1}), where the normalized intensities of this line for two different apertures of the diaphragm are plotted as a function of B. Clearly the 'intensity oscillations' will fade away with increasing field and increasing aperture. Again, the E_g modes are independent of the field.

These intensity anomalies will not occur if only one normal wave, i.e. a circularly polarized wave, enters the crystal along $\hat{Z}$. This becomes evident from Fig. 7, which also illustrates the problems which may occur in investigating scattering cross-sections in gyrotropic materials without selection of proper normal waves. Interesting

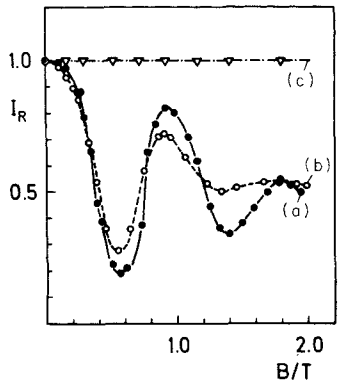

Figure 6. Dependence of normalized Raman intensities, I_R, of different lines [(a, b) A_{1g} (899 cm^{-1}); (c) E_g (843 cm^{-1})] in $TmVO_4$ with magnetic field $\mathbf{B} \| \hat{Z}$ for different lengths of entrance slit: (a) 2 mm; (b) 3 mm; (c) 2 mm. $T = 1.6$ K.

effects of genuine field-dependent Raman cross-sections, where these precautions have to be considered, exist, e.g. in substances with strong interactions between localized $4f$ electrons and phonons.[23,24]

More generally, such intensity effects are also observed under conditions of resonance-enhanced Raman scattering in the vibrational spectra of organic molecules, especially in solutions of metallo-organic compounds containing transition metal ions. This effect, the magnetic Raman optical activity, is observed as the intensity difference between the scattered spectra polarized linearly and observed perpendicularly to the magnetic field B and excited by either right or left circular polarized light, which is propagating parallel to B, i.e. in the Faraday configuration. Although the effects in randomly oriented molecules in a solvent are much smaller than in single crystals, this technique is well established[25] and provides a considerable insight into the electronic and vibrational states of molecules.

Molecules with a chiral structure, i.e. with a natural gyrotropy, demonstrate similar effects even without a magnetic field both in absorption spectra (vibrational optical activity[26]) and in Raman scattering (natural vibrational Raman optical activity[27]). These fields, their theoretical foundations, instrumental details and experimental results, have been intensively reviewed recently.[25-27]

It is important to note that the use of proper normal waves in Raman spectroscopy not only offers formal advantages but is also of fundamental physical importance. Normal waves propagating in a crystal along directions of symmetry can be classified according to the same i.r. of the crystallographic point group of the crystal as the wavefunctions of excitations to be studied spectroscopically. They will interact accordingly with states of a specific i.r. or with one component only of a degenerate i.r. In Fig. 8 this is demonstrated for the case of an E_g phonon in $TmVO_4$, which is split by a magnetic field $\mathbf{B} \| \hat{Z}$. The two phonon modes are right or left circularly polarized,[12,13] and interact only with the normal wave of proper polarization. In crystals with natural optical activity E modes may also split[9,10] into circularly polarized phonon modes of opposite sense of rotation. This is shown in Fig. 9 for the case of ZnP_2 (point group D_4). This Raman dichroism can be used to study very small energy differences between states of different i.r. Degeneracies raised by morphic effects can especially be studied very accurately: splittings $\Delta E \geq 0.1$ cm^{-1}, i.e. much smaller than the half-widths of the split components, have been resolved accurately.[28]

An example of an electronic Zeeman splitting of Mn^{2+} observed in Raman scattering with circularly polarized light has been reported for $Cd_{1-x}Mn_xTe$.[29] Another example, which demonstrates the gain in spectral resolution achievable by using the correct polarization of incident light and the facilities of a computer-driven spectrometer, is given in Fig. 10, which shows the size

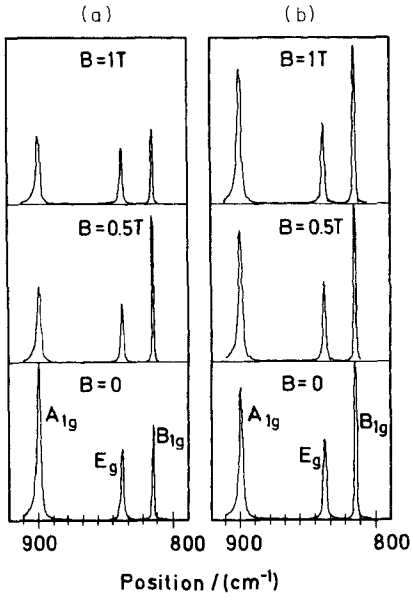

Figure 7. Section of the Raman spectrum of $TmVO_4$ in different magnetic fields B at $T = 1.6$ K. (a) Linear polarization of incident light; (b) circular polarization.

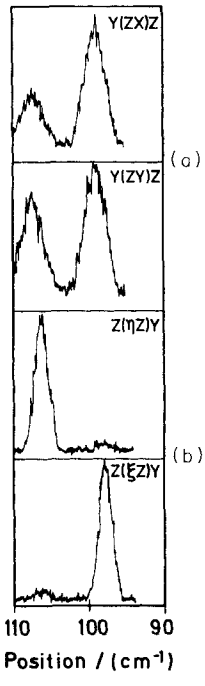

Figure 8. Raman spectra of the two components of an E_g phonon in $TmVO_4$, split by a magnetic field $\hat{Z} \| B = 5$ T; $T = 1.6$ K. (a) Excitation and observation with linearly polarized light; (b) excitation with circularly polarized light (ξ, η), observation with linear polarization.

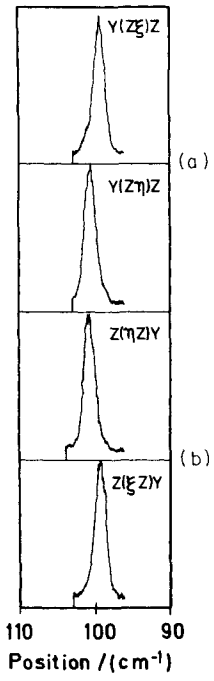

Figure 9. E doublet in the Raman spectra of tetragonal ZnP_2 ($T=300$ K, $\lambda_{exc.}=610$ nm). (a) Excitation with linear polarization, observation with circular polarization; (b) circular excitation, linear observation.

of the splitting ΔE by a magnetic field $\mathbf{B}\|\hat{Z}$ of an E_g phonon at 78 cm^{-1} in CeF_3 (D_{3d}) at $T=2.0$ K. The phonon components have again been resolved by making use of the Raman dichroism of the two phonon components. During a single slow scan of the spectrometer the polarizer of the laser beam was switched by the computer for identical short time intervals between the orthogonal circular polarization (ξ, η). The count rates of both spectra $[Z(\xi, Z)X;\ Z(\eta, Z)X]$ where stored and numerically analysed separately. The solid line in Fig. 10 is a theoretical fit using the function[23,24]

$$\Delta E(B) = \Delta E_S \tanh\left(\frac{g\mu_B H}{k_B T}\right) \qquad (16)$$

where g is the g-factor of the Kramers-degenerate electronic ground state of the Ce^{3+} ion in CeF_3, μ_B is the Bohr magneton, k_B is the Boltzmann constant and ΔE_S is the saturation splitting of this phonon. The half-width (full width at half maximum intensity, FWHM) of both split phonon components is 1.25 cm^{-1}. Obviously, wavenumber shifts as small as 0.03 cm^{-1}, which are spectroscopically accessible in general only by interferometric methods, could be reliably observed in this case.

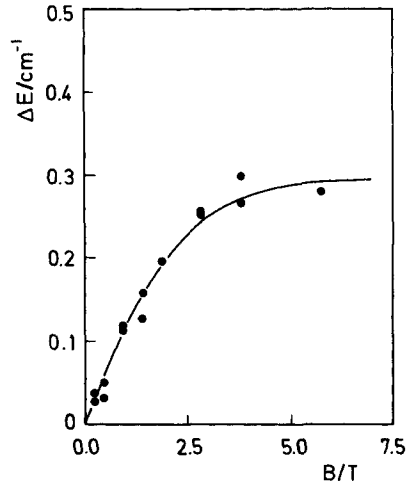

Figure 10. Size of magnetic phonon splitting (E_g, 78 cm^{-1}) in CeF_3. $\mathbf{B}\|\hat{Z}$; $T=2.0$ K.[28]

The use of normal waves for Raman spectroscopic work is even more stringent in the case of absorbing materials. Because of optical dichroism one has to introduce an appropriate absorption constant for each normal wave separately. Formal superposition of the two normal waves in the case of absorption results in elliptical polarization of the light with a complicated evaluation of the polarization ellipse along the light path. The use of a single absorption constant for linearly polarized light which is subject to Faraday rotation, as was assumed in Ref. 4, is not correct.

CONCLUSION

In natural gyrotropic media and in media with gyrotropy induced by external fields there is no breakdown of selection rules for phonon Raman scattering due to gyrotropy. Intensity anomalies obviously occurring in these media can be traced back to interference effects between two normal waves propagating in the crystal either as an exciting or as a scattered wave. These anomalies can be eliminated by the selection of symmetry-adapted normal waves with appropriate polarizers or analysers.

The effects calculated have been demonstrated experimentally in the Raman spectra of quartz with natural optical activity and in paramagnetic $TmVO_4$ in an external magnetic field. For the first time the influence of a magnetic field on the Raman spectrum of a diamagnetic material such as α-quartz has been studied.

REFERENCES

1. R. Loudon, *Adv. Phys.* **13**, 423 (1964); W. Hayes and R. Loudon, *Scattering of Light by Crystals*. Wiley, New York, Chichester (1978).
2. O. G. Vlokh, *JETP Lett.* **13**, 81 (1971).
3. J. F. Nye, *Physical Properties of Crystals*. Clarendon Press, Oxford (1957).
4. Zhang Peng-Xiang and Tu An, *J. Raman Spectrosc.* **14**, 326 (1983).
5. J. F. Scott and S. P. S. Porto, *Phys. Rev.* **161**, 903 (1967).
6. C. M. Hartwig, D. L. Rousseau and S. P. S. Porto, *Phys. Rev.* **188**, 1328 (1969).
7. S. M. Shapiro and J. D. Axe, *Phys. Rev. B* **6**, 2420 (1972).
8. I. S. Gorban', V. P. Grishchuk, V. A. Gubanov, V. M. Moroz, V. F. Orlenko and A. V. Slobodyanyuk, *Sov. Phys. Solid State* **23**, 866 (1981).
9. I. S. Gorban', V. P. Grishchuk, V. A. Gubanov, V. F. Orlenko and

A. V. Slobodyanyuk, *Sov. Phys. Solid State* **24**, 1033 (1982).
10. V. P. Grishchuk, A. V. Slobodyanyuk and Z. Z. Yanchuk, *Sov. Phys. Solid State* **24**, 1767 (1982).
11. V. P. Grishchuk and A. V. Slobodyanyuk, *Ukr. Fiz. Zh.* **27**, 1816 (1982).
12. G. Schaack, *J. Phys. C* **9**, L297 (1976).
13. K. Ahrens and G. Schaack, *Indian J. Pure Appl. Phys.* **16**, 311 (1978).
14. J. O. Dimmock and R. G. Wheeler, in *The Mathematics of Physics and Chemistry II*, edited by H. Margenau and G. M. Murphy. Van Nostrand, New York (1964), p. 786.
15. M. Kerker, *The Scattering of Light and other Electromagnetic Radiation.* Academic Press, New York, London (1969).
16. B. Chu, *Laser Light Scattering.* Academic Press, New York, San Francisco, London (1974).
17. P. J. Becker, M. J. M. Leask and R. N. Tyte, *J. Phys. C* **5**, 2027 (1972).
18. *American Institute of Physics Handbook*, 3rd ed. McGraw-Hill, New York (1972), p. 6–231.
19. A. S. Pine and G. Dresselhaus, *Phys. Rev.* **188**, 1489 (1969).
20. S. P. S. Porto, J. A. Giordmaine and T. C. Damen, *Phys. Rev.* **147**, 608 (1966).
21. L. N. Ovander, *Opt. Spectrosc.* **16**, 735 (1964).
22. G. Placzek, in *Handbuch der Radiologie*, edited by E. Marx, Vol. VI, Part II. Akademie Verlagsgesellschaft, Leipzig (1934), p. 205.
23. K. Ahrens, *Z. Phys. B* **40**, 45 (1980).
24. H. Gerlinger and G. Schaack, *Phys. Rev. B* **33**, 7438 (1986).
25. L. D. Barron and J. Vrbancich, *Adv. Infrared Raman Spectrosc.*, edited by R. J. H. Clark and R. E. Hester, Wiley–Heyden, Chichester, **12**, 215 (1985).
26. L. A. Nafie, *Adv. Infrared Raman Spectrosc.*, edited by R. J. H. Clark and R. E. Hester, Wiley–Heyden, Chichester, **12**, 49 (1985).
27. L. D. Barron and J. Vrbancich, *Top. Curr. Chem.* **123**, 151 (1984).
28. M. Dahl, G. Schaack and B. Schwark, to appear in *Europhysics Lett.* (1987).
29. A. Petrou, D. L. Peterson, S. Venugopalan, R. R. Galazka, A. K. Ramdas and S. Rodriguez, *Phys. Rev. Lett.* **48**, 1036 (1982).